VNU Journal of Science: Earth and Environmental Sciences

Journal homepage: https://js.vnu.edu.vn/EES

Original Article

Moisture Transfer Finite Element Modeling with Soil-Water Characteristic Curve-Based Parameters and its Application to Nhan Co Red Mud Basin Slope

Nguyen Van Hoang[1,*], Hoang Viet Hung[2], Pham Van Dung[2]

[1]*Institute of Geological Sciences-Vietnam Academy of Science and Technology, 84 Chua Lang street, Lang Thuong, Dong Da, Hanoi, Vietnam*

[2]*Thuyloi University - Hanoi Campus, 175 Tay Son, Dong Da, Hanoi, Vietnam*

Received 16 July 2020
Revised 14 December 2020; Accepted 13 February 2021

Abstract: Since the year of 2017, landslides at the red mud basins in Nhan Co alumina factory, Dak Nong province have been occurring during the rainy season. The change of the soil physical and mechanical parameters due to rainwater infiltration has been considered as the main factor of the slope instability. The soil cohesion and angle of internal friction depend greatly on the soil moisture. Specifically, soil with a lower moisture content has a higher shearing strength than that in soil with higher moisture content. The finite element modeling of moisture transfers in unsaturated soils through the relationship between soil moisture, soil suction, unsaturated permeability and soil-moisture dispersivity is capable of accurately predicting the wetting front development. The element sizes and time steps have been selected based on detailed analysis of analytical error estimation and on the numerical simulations with different element sizes numerical simulation errors. Soil samples had been taken then the soil different suctions and corresponding soil moisture values have been determined in the laboratory. The soil water characteristic curve (SWCC) parameters (a, n and m) have been determined by the best fitting using the least squared error method. The hydraulic conductivity of the saturated soil, one of the key input parameters was also determined. The results of the application to the study area's slope has shown that the wetting front depth could be up to 8 meters for 90 days of moisture transfer due to the rainwater infiltration. The wetting front depth and the length of the intermediate part of the moisture distribution curve have increased with the infiltration time. The soil moisture distribution with a depth is an essential information to have soil strength parameters for the slope stability analyses. The slope stability analysis with the soil shear

* Corresponding author.
E-mail address: VDC@yahoo.com

https://doi.org/10.25073/2588-1094/vnuees.4655

strength parameters which are strictly corresponding with the moisture change would provide the most accurate and reliable slope stability results and provide more reliable slope stabilization solutions.

Keywords: Finite element (FE), Unsaturated soil, Soil Water Characteristic Curve (SWCC), Soil-moisture diffusivity, Slope stability.

1. Introduction

The exploitation and processing of mineral resources plays an important role in Vietnam's economy. Since the year of 2000, it has contributed 9.6-10.6% of the country's GDP (Tran Trung Kien and Pham Quang Tu, 2011) [1]. However, in reality, the industry has caused unexpectedly serious adverse consequences to the environment. Two projects on bauxite mining and alumina processing in the Central Highlands of Vietnam started in 2009, i.e., Nhan Co bauxite project in Dak Nong province and Tan Rai project in Lam Dong province. Environmental incidents in the two project sites have occurred continuously.

An overflow of a chemical fluid from the workshop on chemical mixing workshop in August 2011 (dantri.com.vn, 2011) [2] and a leakage of a chemical fluid from a chemical fluid pipe into the surrounding area in February 2016 (tuoitre.vn, 2016) [3] polluted some fish farms and the groundwater. On the 8th October 2014, an incident occurred with the basin of bauxite tailings in Tan Rai bauxite factory in which about 5,000 m^3 of sludge was spilled out into Cai Bang lake, a 10-million-m^3 irrigation reservoir which supplies water for the Tan Rai alumina factory. On the 23rd July 2016, an overflow of a chemical fluid occurred during the testing operation of Nhan Co alumina factory, as a consequence, 9.58 m^3 of the chemical fluid was partly spilled into the Dak Yao stream (Figure 1).

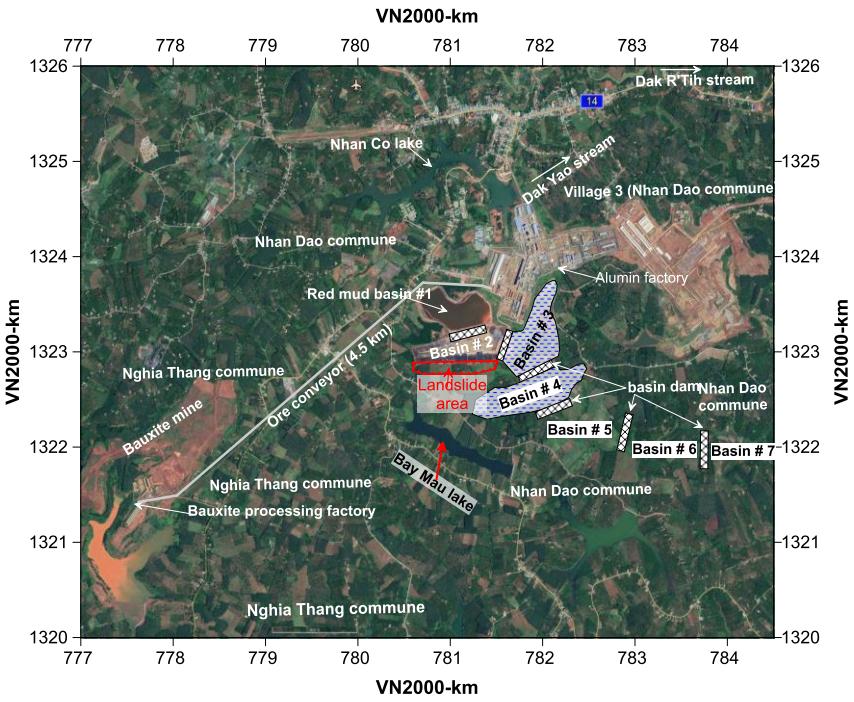

Figure 1. Nhan Co alumina factory, bauxite mine, red mud basins and landslide area.

Seven red mud basins (numbering from 1 to 7) (Figure 1) have been designed for the Nhan Co alumina factory (Vinacomin, 2013) [4] with the total volume of 17.3 millions of cubic meters. At the present, only the red mud basin No. 1 with capacity of 0.26 millions of cubic meters is under operation. However, since August 2017 a series of landslides has been occurring in the neighboring farming land (Figure 2) along the red mud basin No. 2 during 2017 - 2019 rainy seasons, which lead to a complete destruction of transportation road along the red mud basin (Figure 3). In the near future when the red mud basin No. 2 and others are launched into operation, the landslides would definitely cause a possible overflow of the highly toxic fluid to the surrounding environment.

Figure 2. 2018 landslide in farming slope in the red mud basin No. 2 - Nhan Co alumina factory.

Figure 3. 2019 landslide on a road along the red mud basin No. 2 - Nhan Co alumina factory.

As rain occurs, soil moisture increases because of the infiltration of the rainwater. The increased soil moisture leads to the decrease in the soil strength, i.e., cohesion and angle of internal friction. This was quantitatively presented by Robert and Raymond (1978) [5] in Figure 4 which also shows a sharp decrease in the soil strength when the soil changes into plastic and soft condition. Even, for the soil materials from many parts of the world which are used for compacted subgrade under the foundation of engineering structures, there is a strong inverse relationship between the soil shear strength and liquidity index (Karl Terzaghi et al., 1996) [6]. Zhang Huzhu et al. (2017) [7] used the soil from a construction site of the Beijing-Harbin high way to create different soil samples with different degrees of compaction and moisture. The soil samples with the lowest compaction degree (85%) are more or less corresponding to natural soil compaction, both the cohesion and angle of internal friction have an inverse relationship with the water content. The cohesion (c) is decreased from 32 kPa to 9 kPa and the angle of internal friction (ϕ) is decreased from 5^o to 0.2^o when the water content (W) increases from 9% to 21.5%, i.e., $c \approx 48.56\text{-}1.84W$ and $\phi \approx 8.5\text{-}0.38W$.

Therefore, the determination of the moisture distribution in the slope soil due to rainwater infiltration is important in order to have the soil strength parameters which are required in geotechnical analysis such as filtration deformation and slope stability analyses.

2. Moisture transfer modeling in unsaturated zones

2.1. Moisture transfer equation

The equation describing the moisture transfer in a unsaturated soil with an assumption that air does not move is as follows (Pelageia Iakovlevna Polubarinova-Kochina, 1977) [8]:

$$\frac{\partial \upsilon_x}{\partial x} + \frac{\partial \upsilon_y}{\partial y} + \frac{\partial \upsilon_z}{\partial z} = -\frac{\partial \theta_w}{\partial t} \quad (1)$$

In which: θ_w is volumetric water content (VWC); t is time; υ_x, υ_y and υ_z are moisture transfer rates in x, y and z directions, respectively:

$$\upsilon_x = -K(\theta_w)\frac{\partial h}{\partial x};\quad \upsilon_y = -K(\theta_w)\frac{\partial h}{\partial y};$$
$$\upsilon_z = -K(\theta_w)\frac{\partial h}{\partial z} = -K(\theta_w)\left(\frac{\partial \psi}{\partial z}+1\right) \quad (2)$$

Equations (1) and (2) give:

$$\frac{\partial \theta_w}{\partial t} = \frac{\partial}{\partial x}\left(\frac{K(\theta_w)}{\gamma}\frac{\partial h}{\partial x}\right)+\frac{\partial}{\partial y}\left(\frac{K(\theta_w)}{\gamma}\frac{\partial h}{\partial y}\right) + \frac{\partial}{\partial z}\left(\frac{K(\theta_w)}{\gamma}\frac{\partial h}{\partial z}\right) \quad (3)$$

In which: $h=\psi/\gamma+z$; h is a total head; ψ is a soil suction; γ is a water density; and $K(\theta_w)$ is a hydraulic conductivity of unsaturated soil.

$$\frac{\partial \theta_w}{\partial t} = \frac{\partial}{\partial x}\left(\frac{K(\theta_w)}{\gamma}\frac{\partial \psi}{\partial x}\right)+\frac{\partial}{\partial y}\left(\frac{K(\theta_w)}{\gamma}\frac{\partial \psi}{\partial y}\right) + \frac{\partial}{\partial z}\left(\frac{K(\theta_w)}{\gamma}\left[\frac{\partial \psi}{\partial z}+\frac{\partial z}{\partial z}\right]\right) \quad (4)$$

Which is the Richards equation in terms of suction pressure (Richards, 1931) [9].

With water density equal to one and suction pressure ψ as a function of VWC θ_w, Eq. 3 becomes in vertical direction z:

$$\frac{\partial \theta_w}{\partial t} = \frac{\partial}{\partial z}\left(K(\theta_w)\frac{d\psi}{d\theta_w}\frac{\partial \theta_w}{\partial z}+K(\theta_w)\right) \quad (5)$$

The component $D(\theta_w) = K(\theta_w)d\psi/d\theta_w$ is called soil-moisture diffusivity (Philip, 1969) [10] (as cited by Gilding, 1991) [11] with the unit L^2T^{-1}, and then Eq. 5 has the following form*:*

$$\frac{\partial \theta_w}{\partial t} = \frac{\partial}{\partial z}\left[D(\theta_w)\frac{\partial \theta_w}{\partial z}\right]+\frac{\partial K(\theta_w)}{\partial z} \quad (6)$$

The solution of Eq. 6 is subject to initial and boundary conditions.

2.2. Finite element modeling of soil moisture transfer in unsaturated soil

The finite element (FE) method (Zienkiewics and Morgan, 1983) [12] can be applied in solving Eq. 6 with the use of quadratic element shape functions for superior accurate numerical solution than the use of linear shape functions. For simplicity let us use D_z instead of $D_z(\theta_w)$. Applying Green lemma to Eq. 6 with the approximation of water content $\theta_w \approx \hat{\theta}_w = \sum_{m=1}^{M}\theta_{w,m}N_m$ gives:

$$\int_\Omega\left(D_z\frac{\partial^2\hat{\theta}_w}{\partial z^2}\right)W_l dz+\frac{\partial K(\theta_w)}{\partial z} = -\int_\Omega\left(D_z\frac{\partial\hat{\theta}_w}{\partial z}\frac{\partial W_l}{\partial z}\right)dz + \int_\Gamma\left(D_z\frac{\partial\hat{\theta}_w}{\partial z}W_l\mathbf{N}_z\right)d\Gamma+\frac{\partial K(\theta_w)}{\partial z} = \frac{\partial\theta_w}{\partial t} \quad (7)$$

The boundary integration $\int_\Gamma$ is present only for the elements having sides on boundaries Γ_{g_w}:

$$-\int_\Omega\left(D_z\frac{\partial\hat{\theta}}{\partial z}\frac{\partial W_l}{\partial z}\right)dz + \int_{\Gamma_q}\left(D_z\frac{\partial\hat{\theta}}{\partial z}W_l\mathbf{N}_z\right)d\Gamma+\frac{\partial K(\theta_w)}{\partial z} = \frac{\partial\theta_w}{\partial t} \quad (8)$$

Putting $\theta_w \approx \hat{\theta}_w = \sum_{m=1}^{M}\theta_{w,m}N_m$ into (8) results in:

$$-\int_\Omega\left(D_z\frac{\partial N_m}{\partial z}\frac{\partial W_l}{\partial z}\theta_m\right)dz + \int_{\Gamma_q}\left(\bar{q}_c W_l\mathbf{N}_z\right)d\Gamma+\frac{\partial K(\theta_w)}{\partial z} = \frac{\partial\theta_w}{\partial t} \quad (9)$$

$$\mathbf{K} = \int_\Omega\left(D_z\frac{\partial N_m}{\partial z}\frac{\partial W_l}{\partial z}\right)dz; \quad (10)$$

$$\mathbf{f} = \frac{\partial K(\theta_w)}{\partial z}+\int_{\Gamma_q}\left(\bar{q}_c W_l\mathbf{N}_z\right)d\Gamma$$

$$\mathbf{K\theta}+\frac{\mathbf{d\theta}}{\mathbf{dt}} = \mathbf{f} \quad (11)$$

Applying finite element procedure to Eq. 11 for the time domain the following is obtained:

$$\left(\frac{1}{\Delta t_n}+\lambda\mathbf{K}\right)\boldsymbol{\theta}^n+\left[-\frac{1}{\Delta t_n}+(1-\lambda)\mathbf{K}\right]\boldsymbol{\theta}^{n+1} = (1-\lambda)\mathbf{f}^n+\lambda\mathbf{f}^{n+1} \quad (12)$$

Where: λ=0÷1

Zienkiewics and Morgan (1983) [12] in very details showed that the schemes with $\lambda\geq0.5$ are always unconditionally stable for any values of time step Δt.

2.3. Soil moisture transfer modeling with SWCC-based parameters

The first equation describing the relationship between soil moisture content θ_w and soil suction ψ was proposed by Gardner (1958) [13] (as cited by Fredlund and Xing 1994) [14].

$$\theta_w = \frac{\theta_s}{1 + a\psi^n} \quad (13)$$

In which: θ_w is the soil moisture content, θ_S is the saturated soil moisture content, ψ is the soil suction; and a and n are fitting soil parameters associated with the SWCC.

Fredlund and Xing (1994) [14] proposed an equation expressed as:

$$\theta_w = C(\psi)\frac{\theta_S}{\left[\ln\left\{e + (\psi / a)^n\right\}\right]^m} \quad (14)$$

Where: $C(\psi) = 1 - \frac{\ln(1+\psi/\psi_r)}{\ln(1+10^6/\psi_r)}$ is a correction factor; ψ_r is the suction corresponding to the soil residual water content; a is the fitting parameter related to the air-entry value of the soil (kPa); n is the fitting parameter related to the slope of the SWCC; m is the fitting parameter related to the soil residual water content; e=2.71828; ψ is the soil suction (kPa). As Leong and Rahardjo (1997) [16] concluded that $C(\psi)$ can be assumed to be unity without affecting the initial portion of the SWCC, which helps to reduce the number of parameters in the equation, i.e.,:

$$\theta_w = \frac{\theta_S}{\left[\ln\left\{e + (\psi / a)^n\right\}\right]^m} \quad (15)$$

The unsaturated permeability $K(\theta_w)$ of the soil can be determined through relative coefficient of permeability ($k_r(\theta)$) (Fredlund et al. 1994) [15]:

$$K(\theta_w) = K \times k_r(\theta);$$
$$k_r(\theta) = \int_{\theta_L}^{\theta} \frac{\theta - \zeta}{\psi^2(\zeta)} d\zeta \Big/ \int_{\theta_L}^{\theta_S} \frac{\theta_S - \zeta}{\psi^2(\zeta)} d\zeta \quad (16)$$

Where: K is the hydraulic conductivity of saturated soil; θ is the effective VWC defined as $\theta = \theta_w - \theta_r$; θ_w is the VWC; θ_L is the lowest VWC on experimental SWCC; θ_r is the residual VWC; θ_S is the saturated VWC; ζ is a dummy integration variable; $S_e = (\theta_w - \theta_r)/(\theta_S - \theta_r)$ is the effective saturation.

2.4. Procedure of FE modeling of soil moisture transfer with SWCC-based parameters

Fortran programming code of groundwater modeling by finite element method using linear and higher order element functions (Nguyen Van Hoang, 2018) [17] transfer in this work in accordance with the flow chart in Figure 4 with required parameters derived from SWCC function.

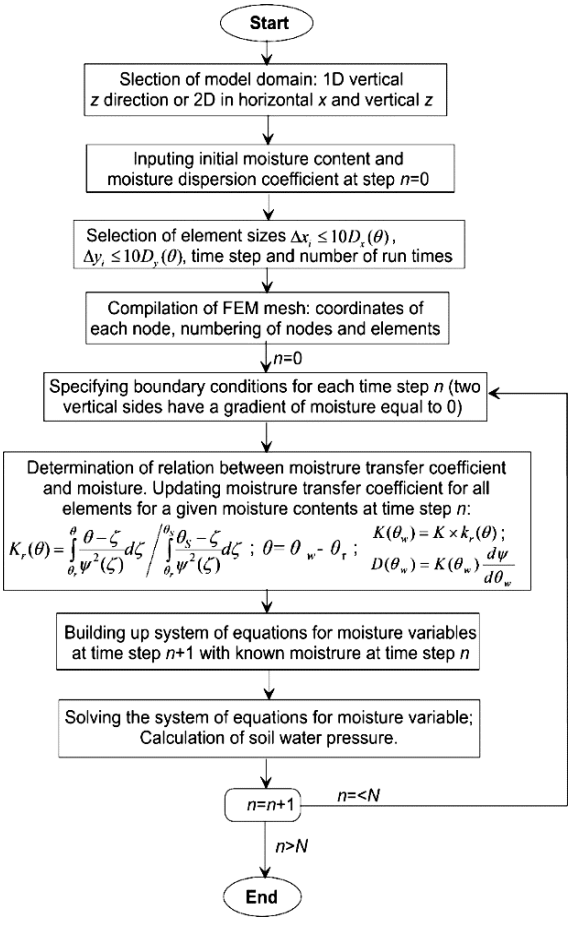

Figure 4. Flow chart of moisture transfer FE modeling with SWCC-based parameters.

Several subroutines have been programmed to determine all the necessary SWCC-based parameters (relationships between the soil suction, relative permeability, soil-moisture diffusivity and VWC), which are required in the soil moisture modeling in accordance with above-described theoretical fundamentals.

3. Physical properties and SWCC parameters of the slope soil

The slope soil in the study is brownish yellow clay with the thickness up to 35 m (Nhan Co alumina joint stock company, 2009) [18]. A field investigation was carried out to collect undisturbed soil samples in the January 2019, the beginning of dry season. The laboratory test for determining the hydraulic conductivity and SWCC of the soil had been carried out in the geotechnical and environmental laboratory (LAS - XD 381) at Thuyloi University, Hanoi [19]. The hydraulic conductivity test is in accordance with the National technical standard TCVN 8723:2012 [20]. The SWCC test procedure is in accordance with the method B and C of the standard ASTM (2002) [21] and described by Nguyen Thi Ngoc Huong and Trinh Minh Thu (2013) [22] is as follows. Soil cylindrical specimens 62 mm in diameter and 20 mm in height were prepared. In order to saturate the soil sample specimens, the two ends of the soil sampling rings containing soil specimens covered by paper filters and porous plates are placed in the test champers of the one-dimensional consolidation testing apparatuses. Water is slowly poured into the chambers to submerge the soil specimens. A loading stress of 10 kN/m^2 is applied over the soil specimens to prevent from possible swelling. The time for saturating the soil specimens is about 48 hours. The saturated soil specimens were subjected to different external air suction pressure values (10 kPa, 20 kPa, 50 kPa, 100 kPa, 200 kPa and 400 kPa). For each of the suction pressure values, the soil pore air suction pressure increases with time and water escapes from the soil specimen through the receiving ceramic discs due to the increased suction. The soil specimen weight is recorded in each time about 24 hours until the weight becomes constant. The volumetric water content (θ) is calculated for each of the suction pressure values.

Table 1. Some physical properties and hydraulic conductivity of the soil

Moisture content (%)	VWC (m^3/m^3)	Wet unit weight (T/m^3)	Dry unit weight (T/m^3)	Degree of saturation (%)	Porosity (%)	K (m/d)
40.42	0.481	1.67	1.19	86.91	55.32	0.0538

Table 2. Results of the laboratory SWCC test

No.	Suction (kPa)	VWC (m^3/m^3)
1	1	0.607
2	10	0.575
3	20	0.551
4	30	0.527
5	50	0.470
6	100	0.366
7	200	0.243
8	300	0.178
9	400	0.150

Some physical properties and hydraulic conductivity of the soil are given in Table 1 and that of SWCC are given in Table 2.

The saturated VWC of the soils is taken to be equal to the soil porosity, and the field natural soil moisture is given in table 1. The porosity of the soil is from 0.553 which is within the range 0.33÷0.60 presented by Fetter (2001) [23].

The SWCC parameters (a, n and m in Eq. 15) have been determined by the method of the least squares are presented in table 3. The SWCC best fitting curve is presented in Figure 5 and the relative coefficient of permeability determined by Eq. 16 is presented in Figure 6.

Table 3. SWCC parameters, saturated and initial VWC

SWCC parameters			Saturated VWC	Initial VWC
a	*n*	*m*	θs	θ_0
60	1.10	1.05	0.553	0.481

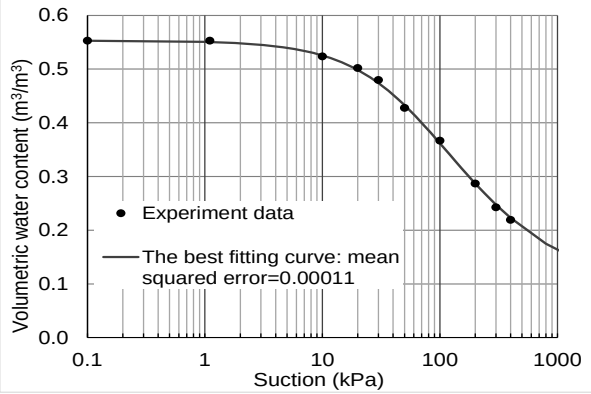

Figure 5. SWCC curve of the modelled soil.

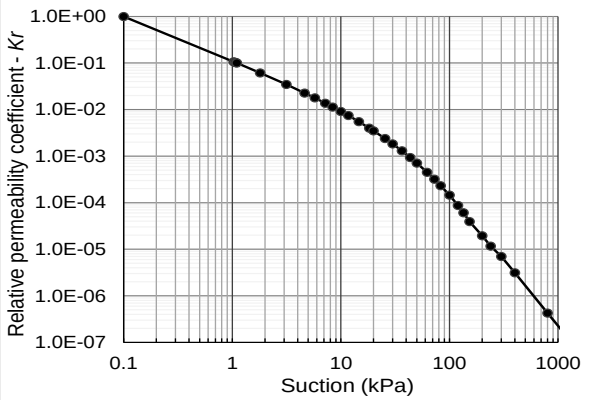

Figure 6. Relative permeability coefficient of the modelled soil.

4. Finite element modeling of the soil moisture transfer in the study site

4.1. Selection of element size in FE modeling

The finite element solutions have a discretization error due to the element size: the smaller element size the less error. For estimating rational element size which ensures a small enough discretization error in our modeling, let us consider the steady state moisture transfer:

$$\frac{\partial}{\partial z}\left[D(\theta_w)\frac{\partial \theta_w}{\partial z}\right]+\frac{\partial K(\theta_w)}{\partial z}=0 \quad (17)$$

The less value of soil-moisture diffusivity, the smaller element size needs to be used as the error estimator for a quadratic element is (Zienkiewics and Morgan, 1983) [12]:

$$\|E\|^2_{\Omega^e}=\frac{\left(h^e\right)^2}{12}\int_0^{h^e} R^2_{\Omega^e}dx \quad (18)$$

In which: Ω^e is the element domain; $R_{\Omega e}$ is the error within the element *e*; h^e is the element size.

Let us consider a hypothetical case with the ratio between permeability gradient and moisture coefficient value equal to 0.01, i.e., the following equation:

$$\partial^2\theta_w/\partial z^2=0.1 \quad (19)$$

If a quadratic element function is used with element size h^e, then the error estimate is:

$$\|E\|^2_{\Omega^e}=\frac{\left(h^e\right)^2}{12}\int_0^{h^e} R^2_{\Omega^e}dx= \frac{\left(h^e\right)^2}{12}\int_0^{h^e} 0.1^2dx=0.01\frac{\left(h^e\right)^2}{12}x\Big|_0^{h^e} \quad (20)$$

The error estimates by Eq. 20 for different elem*ent sizes h^e are presented in Table 4.

Table 4. Error estimates for different element sizes

h^e (m)	0.01	0.02	0.025	0.03125	0.04	0.05
Abs$\|E\|$	0.00003	0.00008	0.00011	0.00015	0.00023	0.00032
Absolute relative maximal VWC error estimate (100×abs Abs$\|E\|$/MinVWC) (%)						
	0.006	0.017	0.024	0.034	0.056	0.079

Therefore, based on the analytical error estimate the element size from 0.01 m to 0.05 m would well meet our modeling accuracy requirement.

Besides the FE discretization modeling error, there are computation round-off error and error due to approximation solution of a system of equations. To access the overall error resulting from discretization, Galerkin FE approximation using quadratic elements is used for Eq. 19. A preliminary analysis had shown that the minimal and maximal values of soil-moisture diffusivity $D(\theta_w)$ are 0.608 m^2/d and 0.01 m^2/d, respectively. Different element sizes from 0.05 m to 0.01 m were used in the simulation of Eq. 19 with element size h^e of 0.01 m, 0.02 m, 0.03125 m, 0.04 m and 0.05 m over a depth of 1 m with VWC of 0.553 m^3/m^3 at the surface and 0.481 m^3/m^3 at the depth of 1 m. Mean squared errors between the numerical results and analytical results have been determined and compared. The soil VWC are presented in Figure 7 and the mean squared errors of all six cases are presented in Figure 8. The most accurate FE result is corresponding to element size of around 0.03125 m with minimal relative error of 0.034%.

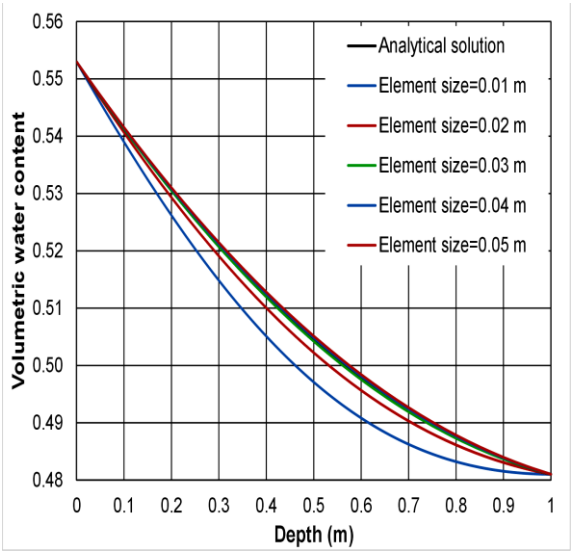

Figure 7. Soil moisture distribution by analytical and numerical solutions with different element sizes.

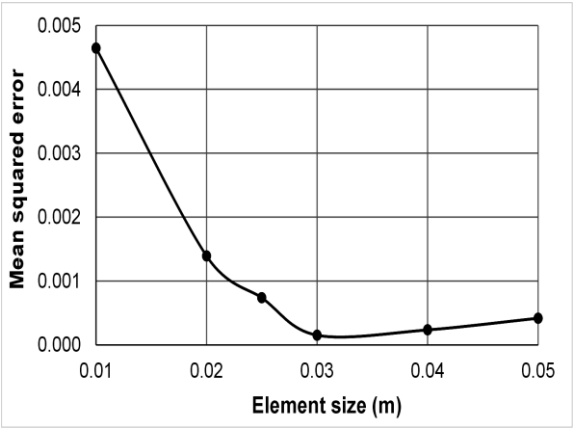

Figure 8. VWC mean squared errors between analytical and FE models with different element sizes.

Regarding the time step, Zienkiewics and Morgan (1983) [12] in very details showed that for our moisture transfer Eq. 5, the most accurate scheme is the Crank-Nicolson scheme (the error order is $O(\Delta t^2)$), and for the forward and backward difference schemes, the time step needs to be:

$$\begin{aligned} &\text{Forward scheme: } \Delta t < \left(h^e\right)^2 / [6D(\theta_w)] \\ &\text{Backward scheme: } \Delta t < \left(h^e\right)^2 / [2D(\theta_w)] \end{aligned} \quad (21)$$

Where the partial differential equation used by Zienkiewics and Morgan (1983) is the same as our moisture transfer equation where $D(\theta_w)$=1. In our work, the Galerkin time scheme is used as recommended by Huyakorn and Pinder (1983) [24] with λ = 2/3 for convection-diffusion equations. With the average soil-moisture diffusivity of 0.1 m^2/d, the element size of 0.03 m and the time step of 3 minutes would be appropriate.

4.2. Initial profile of soil VWC

Initial VWC of the modelled soil profile in the prediction moisture transfer model of the study needs to be determined. The VWC profile of the unsaturated soil layer may be determined by simulation of the model with specified saturated VWC at the bottom of the profile and natural field VWC at the ground surface. The

past studies have showed that the water content had reached a quasi-steady state, i.e., the soil water content almost does not change after several months (Jacob Bear, 2000) [25]. The steady distribution of soil moisture for coarse, fine and very fine soils is described by Jacob Bear (2000) [25] in Figure 9 which shows that for fine soil the moisture is linearly distributed with the depth. With the natural soil moisture of 0.481 m^3/m^3 at the ground surface and 0.553 m^3/m^3 at the depth of 15 m (Table 3 above), the initial VWC of the modeled soil profile were determined by a linear interpolation from the VWC at the surface and the bottom of the profile, while the suctions were determined through VWC and were determined by Eq. 15 with the given SWCC parameters. The initial VWC and suctions are presented in Figure 10. The VWC along the soil profile is presented in the upper abscissa versus the depth in the left ordinate. The suction is presented in the right ordinate versus VWC in the upper abscissa (the VWC and suction at the depth of 5.5 m are illustrated: the horizontal line going through the depth of 5 m and crossing the VWC curve gives VWC of 0.508 on the upper abscissa, the vertical line going through VWC of 0.508 crossing the suction line gives the suction of 16.4 kPa on the right ordinate).

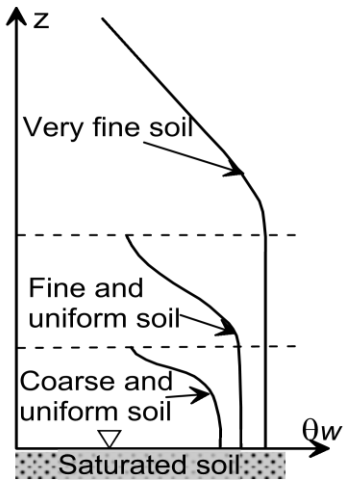

Figure 9. Typical water content profiles for different soils [25].

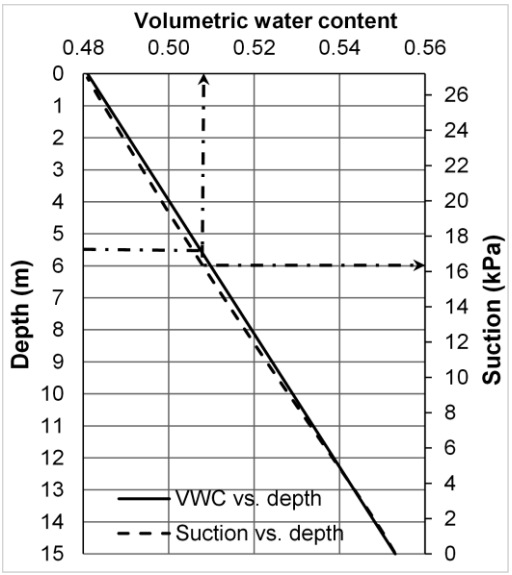

Figure 10. Field initial water content and suction profiles for the modelled soil.

4.3. Boundary conditions

The first-type of boundary condition is assigned to the upper model domain of the ground surface since the moisture transfer model is to be carried out during excessive rainfall events. That is, the soil moisture content at the ground surface is corresponding to the saturated water content. As previously mentioned, during Aug. and Sep. in 2018 and 2019 a series of landslides occurred as a consequence of continuously heavy rain. During the 92 days from 1st Jul. to 30th Sep., there were 92 and 88 rainy days in 2018 and 2019, respectively (Figure 11 and 12) (Dak Nong meteorological station) [26]. It means that it rained almost every day. The average daily rainfall for that period was 18.2 mm and 16.2 mm in 2018 and 2019, respectively.

The lower model domain is also set up as the first-type boundary condition since it directly contacts with below-lying Upper Holocene aquifer. This is also in accordance to many other authors who assigned the boundary as either fixed water table, free drainage (unit gradient), or head dependent (refer to Carrera-Hernández et al., 2012) [27].

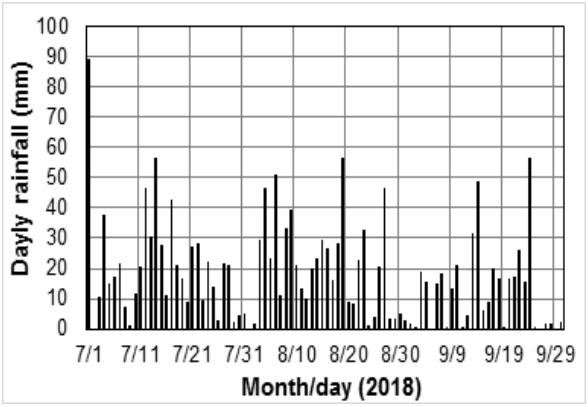

Figure 11. Jul-Sep daily rainfall in 2018 and 2019.

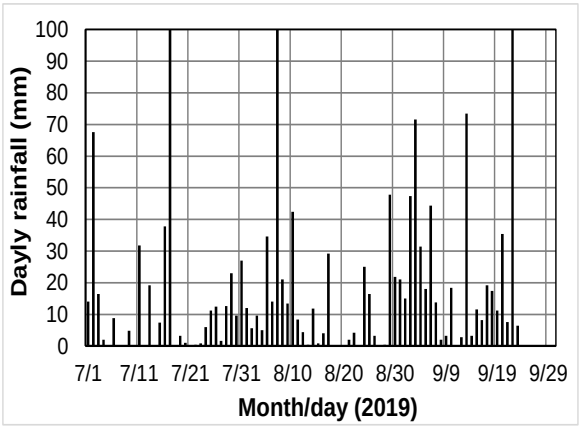

Figure 12. Jul-Sep daily rainfall in 2018 and 2019.

4.4. Simulation results of spatial and temporal soil moisture distribution

The output of the moisture simulation is in the form of moisture content and suction along the depth for a given time interval, e.g., in hours or days. For the purpose of description, a soil moisture distribution curve at a concretely given time is used, or exactly at the 5th day from the beginning of the moisture transfer (Figure 13). For a concretely given time, the moisture distribution curve has three distinguished parts: i) an upper part, from ground surface to the depth Z_1, with a saturated moisture, ii) an intermediate part, from the depth Z_1 to the depth Z_2, with the moisture in between the saturated moisture and a maximal field moisture at Z_2 ($C_{0,Z2}$), and iii) the field moisture from the depth Z_2 and deeper. In the geotechnical analyses such as infiltration deformation and slope stability analyses, the intermediate part of the soil moisture distribution curve is of a special consideration due to the change of the shear strength parameters due to the change of the soil moisture. The upper part of the soil moisture curve has a saturated moisture and would have the shear strength parameters which are corresponding to the saturated soil. The lower part of the soil moisture curve has the natural field moisture, the shear strength parameters of which are correspondingly determined for during the geotechnical investigation

The spatial and temporal soil moisture distribution curves for the whole simulation time of 90 days are presented in Figure 15.

From Figures 13&14 it can be seen that the intermediate part length (from the depth Z_1 to the depth Z_2) increasingly changes with the time of the rainwater infiltration: at the 5th day the length is around 0.82 m and at the 30th day is around 1.2 m (Figure 14). Therefore, for a particular time since the beginning of the moisture transfer due to the rainwater infiltration, a certain length of the intermediate part needs to be specified with moisture for estimation of the soil shear strength parameters for the intended geotechnical analysis.

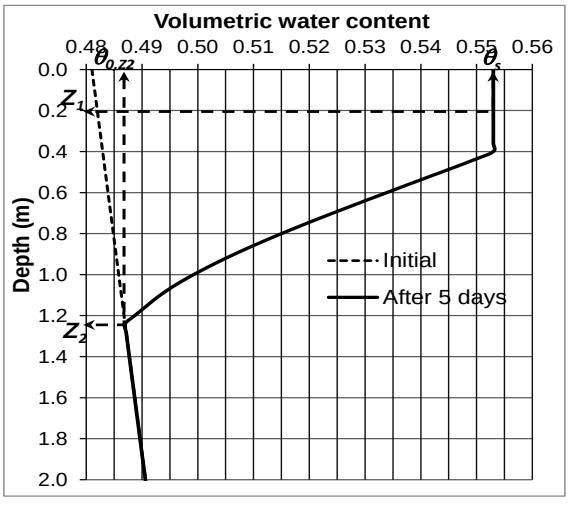

Figure 13. VWC distribution curves for a concretely time at the 5th day.

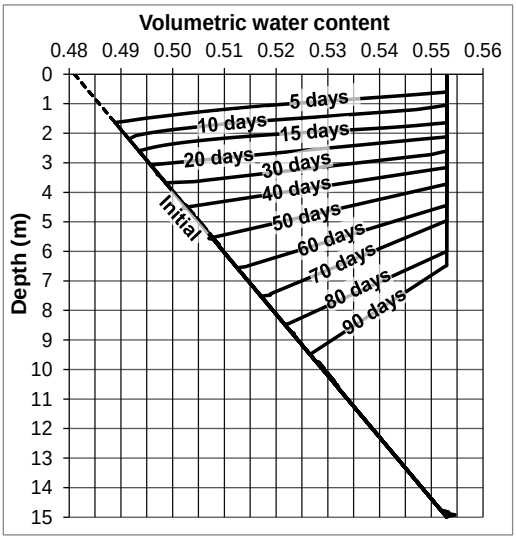

Figure 14. Temporal VWC distribution curves during 90 days.

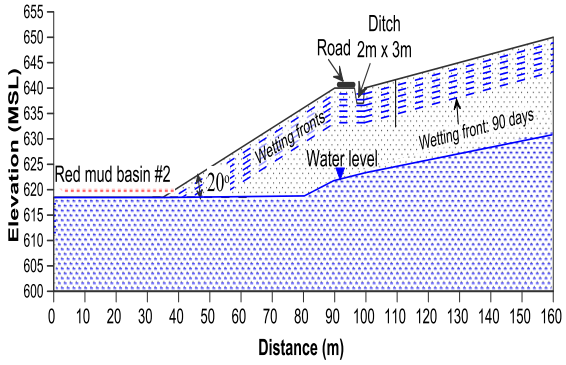

Figure 15. Wetting front curves in the slope along red mud basin No. 2.

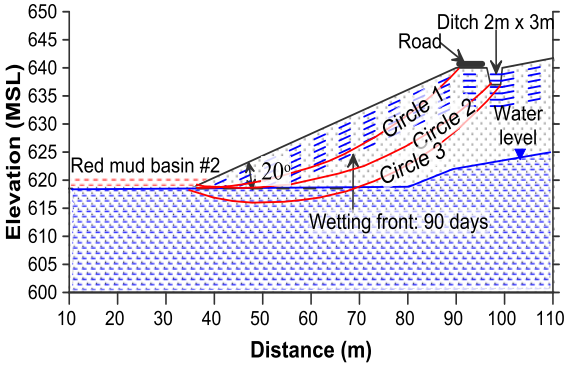

Figure 16. Typical slip circles in regard to soil moisture and groundwater.

Figure 16 presents three typical circles in the slope safety analysis: circle 1 is entirely within the saturated which has lowest shear strength parameters; circle 2 has a long part in the soil mass with a natural field moisture, and circle has a long part in the saturated soil mass with a buoyancy force effect. Among the three circles, circles 1 and 3 would have lowest factor of safety.

5. Concluding remarks

The finite element modeling of simulation of moisture transfer in unsaturated soils is a complicated and powerful tool which is capable of accurately determining the soil moisture distribution in time and space. The SWCC parameters are also time-consuming and expensively determined in the laboratory. Those two aspects in combination are challenging the unsaturated soil mechanics and hydraulics. Those laboratory test experiments and numerical modeling have been carried out for the slope of the red mud basin No. 2 in Nhan Co alumina factory in Dak Nong province.

The SWCC parameters of the study soil are a=60, n=1.10 and m=1.05, which have been determined by the best fitting using the least squared error method, the mean squared error of which is very low and equal to 0.00011. The optimal finite element size for the soil under consideration is around 0.03 m, which had been selected based both on the analytical error estimation and on the numerical simulations with different element sizes. The results of the application to the study area's slope has shown that the wetting front depth can be up to 8 meters for 90 days of moisture transfer in the due to the rainfall. The wetting front depth and the length of the intermediate part of the moisture distribution curve have increased with the infiltration time. The soil moisture distribution with a depth is an essential information to have soil strength parameters for the slope stability analyses. Once, the moisture distribution at a particular time since the beginning of the

moisture transfer due to the rain, the intermediate part of depth needs to be specified with moisture content for the estimation of the soil shear strength parameters for the intended geotechnical slope analysis. The slope stability analysis with the soil shear strength parameters which are strictly corresponding with the moisture change would provide the most accurate and reliable slope stability results and provide more reliable slope stabilization solutions.

There is a limitation matter remains the the study and would be interesting to be studied in derails. The upper boundary condition was set to be the first kind, i.e., a specified constant VWC during the entire modelled time domain based on the reality of 92 days of continuous rainfall, the mean rainfall intensity of which is 16.2 mm ÷ 18.2 mm. The evaporation and excess moisture in the form of condensation for the air temperature drops below its dew point at the ground surface need to be identified for more precise specification of the boundary condition and boundary value of the ground surface. In this case, the upper boundary condition would be specified variable VWC or specified variable moisture flux etc. The effect of the boundary condition and boundary value on the moisture transfer results would assist in selecting a more appropriate boundary condition of the reality,

Acknowledgement

This paper was completed with the support of the project Code KC.08.23/16-20 financed by Ministry of Science and Technology of Vietnam. The authors would like to express a sincere gratitude for the support.

References

[1] T.T. Kien and P.Q. Tu. The role of NGOs in policy criticism: The case of the Consultancy on Development Institute in the sustainable management of mineral resources in Vietnam. Report of the Consultancy on Development Institute (CODE). Ha Noi, Vietnam (2011) (in Vietnamese).

[2] https://dantri.com.vn/kinh-doanh/boxit-tan-rai-tran-hoa-chat-ra-moi-truong-su-co-nho-thiet-hai-lon-1317152926.htm (archived on 24 Sep. 2011) (in Vietnamese).

[3] https://tuoitre.vn/nha-may-boxit-tan-rai-ong-chua-xut-vo-do-lao-hoa-khop-noi-1052089.htm (archived on 16 Feb. 2016) (in Vietnamese).

[4] Vinacomin. Environmental impact assessment for Nhan Co - Dak Nong bauxite mining. Dak Nong, Vietnam (2013) (in Vietnamese).

[5] L. Rober, Schuster and R.J. Krizek. Landslides, analysis and control. National Academy of Sciences, Washington (1978); pp. 234.

[6] K. Terzaghi, R. B. Peck and G. Mesri. Soil mechanics in engineering practice. John Wiley & Sons Inc. (1996). pp. 512.

[7] Z. Huzhu, L.Hanbing, W.Jing and D. Weizhi. Investigation of the effect of water content and degree of compaction on the shear strength of clay soil material. Functional Materials. 24(2) (2017), 290-297. ISSN 1027-5495.

[8] Pelageia Iakovlevna Polubarinova-Kochina. Theory of ground water movement. Publishers "Science" (in Russian) (1977) pp. 664.

[9] L.A. Richards Capillary conduction of liquids through porous mediums, Physics, 1 (1931) 318-333.

[10] J.R. Philip Theory of infiltration. In Advances in Hydroscience Ven Te Chow (editor). Volume 5, Academic Press, New York (1969) 215-296.

[11] B.H. Gilding Qualitative Mathematical Analysis of the Richards Equation. Transport in Porous Media 5(1991) 651-666.

[12] O.C. Zienkiewics and K. Morgan Finite Elements and Approximation. John Willey & Sons (1983) pp. 328.

[13] W.R. Gardner. Some steady state solutions of the unsaturated moisture flow equation with application to evaporation from a water table. Soil Science, 85(1958) 228-232. doi:10.1097/00010694-195804000-00006.

[14] D.G. Fredlund and A. Xing. Equations for the soil-water characteristic curve. Canadian Geotechnical Journal, 31(3) (1994) 521-532.

[15] D.G. Fredlund., A. Xing and S. Huang Predicting the permeability function for unsaturated soils using the soil–water characteristic curve. Canadian Geotechnical Journal, 31(3) (1994) 533–546.

[16] E.C. Leong and R.H. Permeability functions for unsaturated soils. Journal of geotechnical and geoenvironmental engineering. Dec. 1997. (1997) 1118-1126.

[17] N.V. Hoang. Study on building finite element modeling software to simulate groundwater flow and pollutant and salt transport by groundwater-application to the Vietnam Central coast plain. Vietnam NAFOSTED and Vietnam Ministry of Science and Technology. Project's code: ĐT.NCCB-ĐHUD.2012-G/04 (2018) (in Vietnamese).

[18] Nhan Co alumina joint stock company. Environmental impact assessment for Nhan Co alumina factory in Nhan Co commune, Dak R'lap district, Dak Nong province. Dak Nong, Vietnam (2009) (in Vietnamese).

[19] Thuyloi University, Hanoi. http://www.tlu.edu.vn/

[20] TCVN 8723 : 2012. Soil for hydraulic engineering construction - Laboratory test method for determination of permeability coefficient of soil (2012) (in Vietnamese).

[21] ASTM D6836-02: Standard Test Method for Determination of the Soil Water Characteristic Curve for Desorption Using Hanging Column, Pressure Extractor, Chilled Mirror Hygrometer, and/or Centrifuge. Annual Book of ASTM Standards, Volume 04.09 (2002).

[22] N.T.N. Huong and T.M. Thu. Determining shear strength of an unsaturated soil by the direct shear tests. J. of Water Resources & Environmental Engineering 42(9) (2013) (in Vietnamese).

[23] C.W. Fetter. Applied Hydrogeology. Prentice Hall-Upper Saddle River, NJ 07458. (2001) pp. 598.

[24] P.S. Huyakorn and G. F Pinder. Computational method in subsurface flow. Academic Press Inc. (1983) pp. 473.

[25] J Bear. Computer-Mediated Distance Learning Course on modeling groundwater flow and contaminant transport. Topic D: modeling flow in the unsaturated zone (2000). Faculty of Civil Engineering Technion-Israel Institute of Technology. Haifa 32000, Israel.

[26] Dak Nong meteorology station. Monitored daily precipitation of the 2018 and 2019 years. Dak Nong, Vietnam (2020) (in Vietnamese).

[27] J.J. Carrera-Hernández, B.D. Smerdon and C.A. Mendoza. Estimating groundwater recharge through unsaturated flow modeling: Sensitivity to boundary conditions and vertical discretization. Journal of Hydrology 452–453 (2012) 90–101.